

See discussions, stats, and author profiles for this publication at: <https://www.researchgate.net/publication/308989812>

# Prompt gamma imaging of a pencil beam with a high efficiency compton camera at a clinical proton therapy facility

Conference Paper · October 2015

DOI: 10.1109/NSSMIC.2015.7582136

CITATIONS

0

READS

27

9 authors, including:



**J. Petzoldt**

Ion Beam Applications

27 PUBLICATIONS 165 CITATIONS

[SEE PROFILE](#)



**Fine Fiedler**

Helmholtz-Zentrum Dresden-Rossendorf

118 PUBLICATIONS 1,159 CITATIONS

[SEE PROFILE](#)



**Thomas Kormoll**

Technische Universität Dresden

40 PUBLICATIONS 181 CITATIONS

[SEE PROFILE](#)

Some of the authors of this publication are also working on these related projects:



Prompt-gamma based range verification in particle therapy [View project](#)



Positron Annihilation Sepctroscopy [View project](#)

# Prompt Gamma Imaging of a Pencil Beam with a High Efficiency Compton Camera at a Clinical Proton Therapy Facility

F. Hueso-González, J. Petzoldt, K. E. Römer, S. Schöne,  
F. Fiedler, C. Golnik, T. Kormoll, G. Pausch and W. Enghardt

**Abstract**—Protons are excellent particles for tumour treatment due to the increased ionization density close to their stopping point. In practice, the uncertainty on the particle range compromises the achievable accuracy. Compton cameras imaging prompt gamma rays, a by-product of the irradiation, have been proposed for indirect range verification years since. At Universitäts Protonen Therapie Dresden, two BGO block detectors (from PET scanners) arranged as Compton camera are deployed for imaging tests with high energy prompt gamma rays produced in PMMA by a proton pencil beam. Target shifts, thickness increase and beam energy variation experiments are conducted. Each measurement lasts about 15 minutes at a low proton beam current. The effect of one centimetre proton range deviations on the backprojected images is analysed. In conclusion, the experimental results highlight the potential application of Compton cameras for high energy prompt gamma ray imaging of pencil beams, as a real-time and in vivo range verification method in proton therapy.

**Index Terms**—proton therapy, prompt gamma ray imaging, range verification, Compton camera, BGO block detector.

## I. INTRODUCTION

**A**CCCELERATED protons are outstanding particles for cancer treatment thanks to their finite range and the increase of the ionization density (the Bragg peak) close to the stopping point [1]. The dose can be concentrated on the tumour while normal tissue can be spared more efficiently than with traditional photon therapy. In practice, intrinsic proton range uncertainties prevent from fully exploiting these features. The position of the Bragg peak has a critical dependence on tissue composition, which may change inadvertently between treatment fractions. This forces the application of broad safety margins [2] and compromises to some extent the ultimate precision and aspirations of proton therapy.

F. Hueso-González and W. Enghardt are with Helmholtz-Zentrum Dresden - Rossendorf, Institute of Radiooncology, Bautzner Landstr. 400, 01328 Dresden, Germany.

K. E. Römer, S. Schöne and F. Fiedler are with Helmholtz-Zentrum Dresden - Rossendorf, Institute of Radiation Physics, Bautzner Landstr. 400, 01328 Dresden, Germany.

J. Petzoldt, C. Golnik, T. Kormoll, G. Pausch and W. Enghardt are with OncoRay - National Center for Radiation Research in Oncology, Faculty of Medicine and University Hospital Carl Gustav Carus, Technische Universität Dresden, Fetscherstr. 74, PF 41, 01307 Dresden, Germany.

W. Enghardt is also with Department of Radiation Oncology, Faculty of Medicine and University Hospital Carl Gustav Carus, Technische Universität Dresden, Fetscherstr. 74, 01307 Dresden, Germany, and with German Cancer Consortium (DKTK), Dresden, Germany.

Contact: Fernando.Hueso@OncoRay.de. This work was supported by the German Federal Ministry of Education and Research (BMBF-03Z1NN12) and the European Commission (FP7 Grant Agreement N. 264552).

In vivo range verification in real-time is imperative to overcome this limitation and detect severe range deviations. Diverse experimental tools have been proposed during the last decades [3], but none is applied (widespread) in clinical routine yet. Significant efforts are focused on the imaging of prompt  $\gamma$ -rays: a secondary radiation whose emission distribution is correlated to the proton dose deposition. Since the energy spectrum of prompt  $\gamma$ -rays spans over the MeV region, gamma cameras used traditionally in nuclear medicine for lower energies cannot be used here. Systems based on passive collimation, specially designed for the current application, have proven the capability of detecting millimetre range shifts at clinical currents [4] and with heterogeneous phantoms [5].

Compton cameras have been suggested for prompt  $\gamma$ -ray imaging (PGI) as an alternative to the passive collimator years since. A scatterer plane and an absorber detector, with high energy and spatial resolution, as well as photoabsorption efficiency, allow the reconstruction of the incidence direction of  $\gamma$ -rays based on the Compton equation:

$$\begin{aligned}\cos \theta &= 1 - m_e c^2 (1/E_\gamma' - 1/E_\gamma) \\ E_\gamma &= L_s + L_a \\ E_\gamma' &= L_a\end{aligned}\quad (1)$$

where  $E_\gamma$  and  $E_\gamma'$  refer to the initial and final photon energies.  $\theta$  is the dispersion angle,  $m_e$  is the electron mass, and  $L_s$  and  $L_a$  are the energy deposits in each layer, cf. fig. 1.

Detector time resolution is also advisable to reject random coincidences. However, the non-monoenergetic energy spectrum, high  $\gamma$ -ray energies, large detector load and increased radiation background cast doubts on the applicability of this approach in a clinical scenario. As a consequence, a camera prototype demonstrating range verification in a clinical scenario is still a challenge several institutes aim at [6], [7], [8], [9], [10], [11]. To the best of our knowledge, published experimental results are restricted either to 4.4 MeV  $\gamma$ -rays in a background-free scenario [12], to  $< 2$  MeV  $\gamma$ -rays [13], [14] at a proton beam (lower correlation to the range), or to  $> 2$  MeV prompt  $\gamma$ -rays in a proton therapy facility but with beam currents far below the clinical values [15]. There is a need to provide further experimental results, close the gap and assess the suitability of Compton cameras for detecting range shifts at a proton pencil beam by measuring  $> 2$  MeV prompt  $\gamma$ -rays with clinical beam currents. This knowledge would complement the existing simulation studies and might even drive the design of future clinical prototypes.

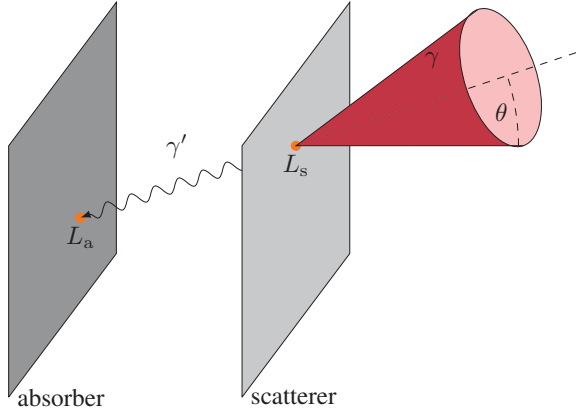


Fig. 1. Incoherent scattering event in a two plane Compton camera. The cone surface contains the possible incidence directions (any generatrix) of the initial photon ( $\gamma$ ). It interacts with the scatterer plane and deposits an energy  $L_s$ . The scattered photon ( $\gamma'$ ) releases the rest of the energy  $L_a$  in the absorber. The line connecting both interaction points (in orange) is the propagation direction of  $\gamma'$ . This defines the axis (directrix) of the aforementioned cone, with half-opening (scattering) angle  $\theta$  and vertex at the scatter point, cf. eq. 1.

## II. AIM

There are few publications concerning experimental tests of the Compton camera at a clinical proton beam. Asymmetry between the rate of scatterer and absorber and small coincident efficiency are common problems, among others. This manuscript presents a Compton camera setup assembled at OncoRay and Helmholtz-Zentrum Dresden - Rossendorf, which is based on two segmented  $\text{Bi}_4\text{Ge}_3\text{O}_{12}$  (BGO) block detectors. The rationale is to maximize the Compton interaction efficiency of the scatterer to the detriment of higher energy resolution but less dense materials. We aim to show experimentally the sensitivity of this camera to range shifts of a proton pencil beam for high energy prompt  $\gamma$ -rays. The effect of target shifts, increase of target thickness and proton energy variation on the reconstructed images is analysed.

## III. MATERIALS AND METHODS

The *BbCc* is a Compton camera setup comprising two BGO block detectors from Siemens Positron Emission Tomography (PET) scanners. The scatterer has a size of  $36.0 \times 39.5 \times 30.0 \text{ mm}^3$ , the absorber of  $52.7 \times 52.7 \times 20.0 \text{ mm}^3$ . Each crystal is segmented in an  $8 \times 8$  matrix and coupled to four light-sharing Photomultiplier Tubes (PMT) operated at +1350 V. The blocks are arranged face-to-face and the distance between the respective crystal centres is  $\sim 6.5 \text{ cm}$ . The signal processing is based on analog front-end electronics [16].

The reason for the relatively high efficiency of this setup, concerning single events, is the dependence of the Compton attenuation coefficient  $\sigma$  on  $\rho/E_\gamma$  [17, chapter 4]. A very dense (and thick) scatterer (BGO has a large mass density  $\rho$ ) is chosen to balance the high energy  $E_\gamma$  expected in the PGI field. To give some numbers, the Compton interaction efficiency  $\epsilon_\sigma = 1 - \exp(-\sigma h)$ , where  $h$  is the scatterer thickness, for the *BbCc* and 4.4 MeV  $\gamma$ -rays yields 40 %.

Previous to beam tests, the *BbCc* is characterized extensively with point-like photon sources:  $^{22}\text{Na}$  (511 and

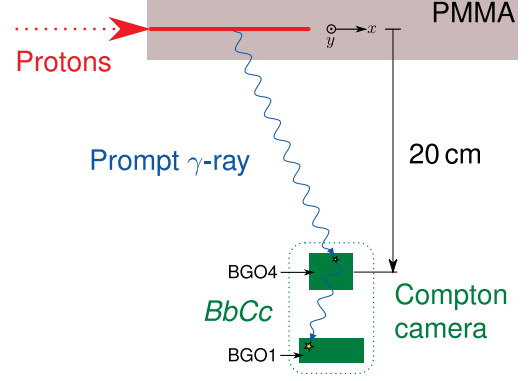
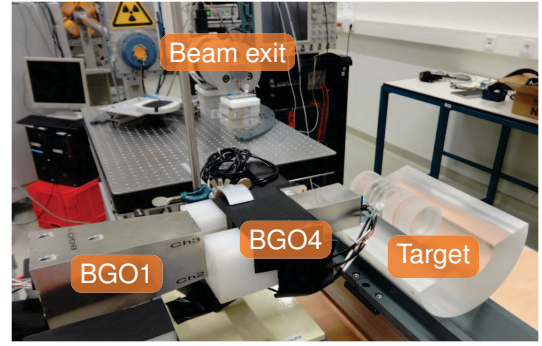


Fig. 2. Photo (top) and schematic top view (bottom) of the *BbCc* setup at the experimental room of UPTD. The protons, with an energy between 70 and 170 MeV, and a repetition rate of 106 MHz, irradiate the homogeneous PMMA target and the *BbCc* setup measures the prompt  $\gamma$ -rays. Real aspect ratio is preserved.

1275 keV),  $^{60}\text{Co}$  (1173 and 1333 keV) and  $^{13}\text{C}$  (6130 keV). A  $^{22}\text{Na}$  line source measurement is acquired by a periodic uniform motion of the point source. The spatial and time resolution of each block is measured as a function of photon energy at the ELBE accelerator. The block detector calibration procedure is detailed in [18].

The camera is then tested at the horizontal pencil beam line (experimental area) of the Universitäts Protonen Therapie Dresden (UPTD). A cylindrical polymethyl methacrylate (PMMA) target is irradiated with low beam currents compared to therapy conditions, since our current acquisition system allows only a limited throughput. The camera is placed perpendicularly to the beam axis at a distance of 20 cm, cf. fig. 2, and detects the produced prompt  $\gamma$ -rays.

Three types of experiments are carried out for exploring the responsiveness of the camera to range deviations: (a) shifts of a 2 cm thick PMMA target along the beam axis for 70 MeV protons, (b) increase of the target thickness in 2 cm steps for 160 MeV protons, (c) variation of the beam energy in 10 MeV steps from 70 to 170 MeV for a 40 cm thick target. Each measurement point lasts around 15 min with a continuous beam current of  $\sim 40 \text{ pA}$  and an individual detector load of  $\sim 50 \text{ kcps}$ .

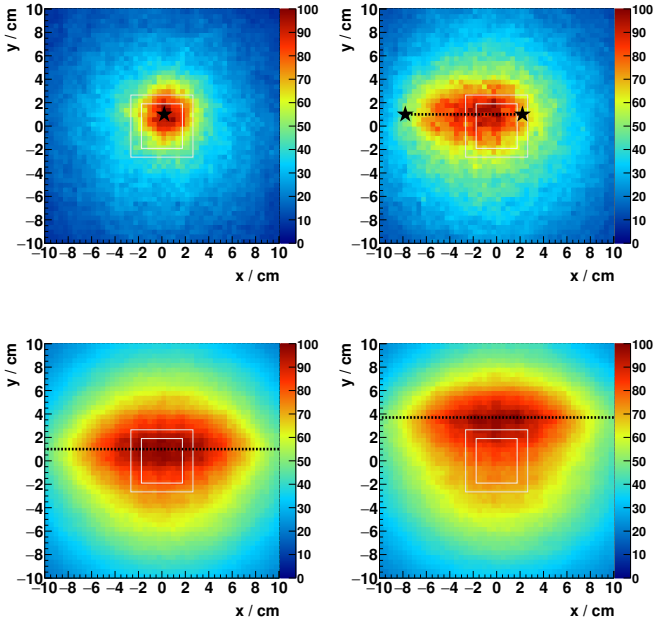


Fig. 3. Back projection images of the *BbCc* at UPTD with a 1275 keV point-like source. Its separation to the scatterer center is  $(18.0 \pm 0.9)$  cm. The white rectangles represent the front faces of the block detectors in the center of the field of view. Top left: the black star is the expected source position. Top right: a 10 cm line source is produced by a periodic motion of the source across the dashed line (between the two black stars). Bottom row: 30 cm line source (see dashed line, black stars are out of the histogram range) at different heights ( $y$  axis) with respect to the camera.

#### IV. RESULTS

Fig. 3 (top left) depicts the back projection of a  $^{22}\text{Na}$  source placed in front of the *BbCc*. No iterative reconstruction algorithm has been applied. The Full Width at Half Maximum is  $\sim 5$  cm on each spatial dimension. Fig. 3 (top right) corresponds to a 10 cm line source, whereas the bottom row is obtained with 30 cm line sources at different heights ( $y$  axis).

Fig. 4 (left) shows the image of a 4.4 MeV prompt  $\gamma$ -ray distribution produced by a 70 MeV proton pencil beam irradiating a 2 cm thick homogeneous PMMA phantom at UPTD. The right plot corresponds to 160 MeV protons on a 40 cm thick target.

Note that, in both cases, an energy filter is applied between 3.0 and 5.0 MeV, to enclose the full energy 4.4 MeV as well as single and double escape peaks. In addition, it is assumed that all filtered events stem from 4.4 MeV  $\gamma$ -rays. The energy deposit  $L_a$  in the absorber is then corrected event-wise for missing energy (due to the photon escape) so that the energy sum  $E_\gamma = L_s + L_a$  yields 4.4 MeV.

The numerical analysis of further experimental data give evidence that range variations around 1 cm can be detected. However, in a clinical scenario, the camera efficiency is not enough to detect these deviations for each spot due to insufficient statistics [19, fig. 19], and the detector load would be unsustainable for BGO (pile-up). The results of the quantitative study will be presented in the full paper.

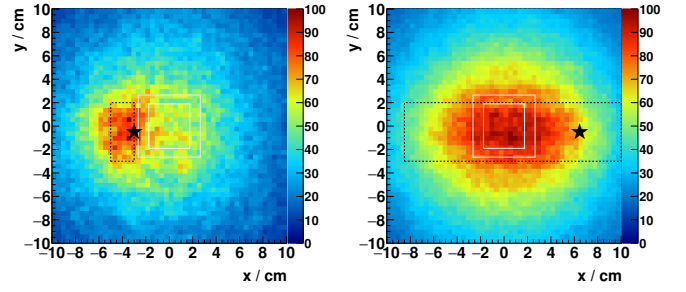


Fig. 4. Backprojection images of the *BbCc* at UPTD corresponding to 4.4 MeV prompt  $\gamma$ -rays of a proton beam on a homogeneous PMMA phantom. Beam incidence is from the left. The distance between beam axis and scatterer center is  $(20.0 \pm 0.9)$  cm. The white rectangles represent the front faces of the block detectors in the center of the field of view. The dashed rectangle represents the target size and the black star, the expected proton range in PMMA. Time and energy filter are applied, and the effect of missing energy is corrected, see text. The proton energies are 70 MeV (left) and 160 MeV (right).

#### V. CONCLUSIONS

Due to technical complexity and high radiation background, only few experimental results hint at the applicability of Compton cameras in a clinical environment. In this paper, we measure with a high efficiency Compton camera 4.4 MeV prompt  $\gamma$ -rays produced in a PMMA phantom when irradiated by a proton pencil beam. Low currents are chosen to adapt the count rate to the throughput of our acquisition system.

Target shifts, thickness increase or beam energy variation, corresponding to range differences down to 1 cm, correlate to changes of the back projected images. This preliminary analysis highlights the ability of the *BbCc* to image high energy prompt  $\gamma$ -rays, despite the moderate energy resolution of BGO.

However, the high detector rates and low statistics collected per spot in a realistic treatment plan (based on estimates with pencil beam scanning and clinical currents) question the feasibility of the Compton camera as in vivo real-time range verification.

#### ACKNOWLEDGEMENT

We thank M. Berthel, A. Dreyer, K. Heidel, S. Helmbrecht, M. Iltzsche, M. Priegnitz, M. Sobiella, A. Wagner and D. Weinberger for the excellent support and the crew of the UPTD accelerator for stable operations.

## REFERENCES

- [1] R. R. Wilson, "Radiological use of fast protons," *Radiology*, vol. 47, no. 5, p. 487, 1946. [Online]. Available: <http://dx.doi.org/10.1148/47.5.487>
- [2] H. Paganetti, "Range uncertainties in proton therapy and the role of monte carlo simulations," *Phys. Med. Biol.*, vol. 57, no. 11, p. R99, 2012. [Online]. Available: <http://dx.doi.org/10.1088/0031-9155/57/11/R99>
- [3] A.-C. Knopf and A. Lomax, "In vivo proton range verification: a review," *Phys. Med. Biol.*, vol. 58, no. 15, p. R131, 2013. [Online]. Available: <http://dx.doi.org/10.1088/0031-9155/58/15/R131>
- [4] I. Perali, A. Celani, L. Bombelli, C. Fiorini, F. Camera, E. Clementel, S. Henrotin, G. Janssens, D. Prieels, F. Roellinghoff, J. Smeets, F. Stichelbaut, and F. V. Stappen, "Prompt gamma imaging of proton pencil beams at clinical dose rate," *Phys. Med. Biol.*, vol. 59, no. 19, p. 5849, 2014. [Online]. Available: <http://dx.doi.org/10.1088/0031-9155/59/19/5849>
- [5] M. Priegnitz, S. Helmbrecht, G. Janssens, I. Perali, J. Smeets, F. V. Stappen, E. Sterpin, and F. Fiedler, "Measurement of prompt gamma profiles in inhomogeneous targets with a knife-edge slit camera during proton irradiation," *Phys. Med. Biol.*, vol. 60, no. 12, p. 4849, 2015. [Online]. Available: <http://dx.doi.org/10.1088/0031-9155/60/12/4849>
- [6] T. Kormoll, F. Fiedler, S. Schöne, J. Wüstemann, K. Zuber, and W. Enghardt, "A compton imager for in-vivo dosimetry of proton beams - a design study," *Nucl Instrum Methods Phys Res A*, vol. 626-627, no. 0, pp. 114–119, 2011. [Online]. Available: <http://dx.doi.org/10.1016/j.nima.2010.10.031>
- [7] H. Seo, J. H. Park, A. Ushakov, C. H. Kim, J. K. Kim, J. H. Lee, C. S. Lee, and J. S. Lee, "Experimental performance of double-scattering compton camera with anthropomorphic phantom," *J Instrum*, vol. 6, no. 01, p. C01024, 2011. [Online]. Available: <http://dx.doi.org/10.1088/1748-0221/6/01/C01024>
- [8] G. Llosá, J. Cabello, S. Callier, J. Gillam, C. Lacasta, M. Rafecas, L. Raux, C. Solaz, V. Stankova, C. de La Taille, M. Trovato, and J. Barrio, "First compton telescope prototype based on continuous labr3-sipm detectors," *Nucl Instrum Methods Phys Res A*, vol. 718, no. 0, pp. 130–133, 2013. [Online]. Available: <http://dx.doi.org/10.1016/j.nima.2012.08.074>
- [9] J. Krimmer, J.-L. Ley, C. Abellan, J.-P. Cachemiche, L. Caponetto, X. Chen, M. Dahoumane, D. Dauvergne, N. Freud, B. Joly, D. Lambert, L. Lestand, J. Létang, M. Magne, H. Mathez, V. Maxim, G. Montarou, C. Morel, M. Pinto, C. Ray, V. Reithinger, E. Testa, and Y. Zoccarato, "Development of a compton camera for medical applications based on silicon strip and scintillation detectors," *Nucl Instrum Methods Phys Res A*, vol. 787, pp. 98–101, 2014. [Online]. Available: <http://dx.doi.org/10.1016/j.nima.2014.11.042>
- [10] P. Thirolf, C. Lang, S. Aldawood, H. v.d. Kolff, L. Maier, D. Schaart, and K. Parodi, "Development of a compton camera for online range monitoring of laser-accelerated proton beams via prompt-gamma detection," *EPJ Web of Conferences*, vol. 66, no. 11036, 2014. [Online]. Available: <http://dx.doi.org/10.1051/epjconf/20146611036>
- [11] M. McCleskey, W. Kaye, D. Mackin, S. Beddar, Z. He, and J. Polf, "Evaluation of a multistage cdznte compton camera for prompt  $\gamma$  imaging for proton therapy," *Nucl Instrum Methods Phys Res A*, vol. 785, no. 0, pp. 163–169, 2015. [Online]. Available: <http://dx.doi.org/10.1016/j.nima.2015.02.030>
- [12] T. Kormoll, C. Golnik, S. Akhmadaliev, D. Bemmerer, J. Borany, F. Fiedler, F. Hueso González, K. Heidel, M. Kempe, H. Rohling, K. Schmidt, S. Schone, L. Wagner, and G. Pausch, "Compton imaging in a high energetic photon field," in *IEEE Nucl Sci Symp Conf Rec*, vol. M19-3, 2013, pp. 1–3. [Online]. Available: <http://dx.doi.org/10.1109/NSSMIC.2013.6829302>
- [13] S. Kabuki, K. Ueno, S. Kurosawa, S. Iwaki, H. Kubo, K. Miuchi, Y. Fujii, D. Kim, J. Kim, R. Kohara, O. Miyazaki, T. Sakae, T. Shirahata, T. Takayanagi, T. Terunuma, Y. Tsukahara, E. Yamamoto, K. Yasuoka, and T. Tanimori, "Study on the use of electron-tracking compton gamma-ray camera to monitor the therapeutic proton dose distribution in real time," in *IEEE Nucl Sci Symp Conf Rec*, vol. J05-13, 2009, pp. 2437–2440. [Online]. Available: <http://dx.doi.org/10.1109/NSSMIC.2009.5402130>
- [14] S. Kurosawa, H. Kubo, K. Ueno, S. Kabuki, S. Iwaki, M. Takahashi, K. Taniue, N. Higashi, K. Miuchi, T. Tanimori, D. Kim, and J. Kim, "Prompt gamma detection for range verification in proton therapy," *Curr Appl Phys*, vol. 12, no. 2, pp. 364–368, 2012. [Online]. Available: <http://dx.doi.org/10.1016/j.cap.2011.07.027>
- [15] J. C. Polf, S. Avery, D. S. Mackin, and S. Beddar, "Imaging of prompt gamma rays emitted during delivery of clinical proton beams with a compton camera: feasibility studies for range verification," *Phys. Med. Biol.*, vol. 60, no. 18, p. 7085, 2015. [Online]. Available: <http://dx.doi.org/10.1088/0031-9155/60/18/7085>
- [16] F. Hueso González, C. Golnik, M. Berthel, A. Dreyer, W. Enghardt, F. Fiedler, K. Heidel, T. Kormoll, H. Rohling, S. Schöne, R. Schwengner, A. Wagner, and G. Pausch, "Test of compton camera components for prompt gamma imaging at the elbe bremsstrahlung beam," *J Instrum*, vol. 9, no. 05, p. P05002, 2014. [Online]. Available: <http://dx.doi.org/10.1088/1748-0221/9/05/P05002>
- [17] H. Krieger, *Strahlenphysik, Dosimetrie und Strahlenschutz*. Vieweg+Teubner Verlag, 1998, vol. 1, pp. 112–162. [Online]. Available: [http://dx.doi.org/10.1007/978-3-663-11534-2\\_4](http://dx.doi.org/10.1007/978-3-663-11534-2_4)
- [18] F. Hueso González, A. K. Biegun, P. Dendooven, W. Enghardt, F. Fiedler, C. Golnik, K. Heidel, T. Kormoll, J. Petzoldt, K. E. Römer, R. Schwengner, A. Wagner, and G. Pausch, "Comparison of Iso and bgo block detectors for prompt gamma imaging in ion beam therapy," *J Instrum*, vol. 10, no. 9, p. P09015, 2015. [Online]. Available: <http://dx.doi.org/10.1088/1748-0221/2015/9/P09015>
- [19] J. Smeets, F. Roellinghoff, D. Prieels, F. Stichelbaut, A. Benilov, P. Busca, C. Fiorini, R. Peloso, M. Basilavecchia, T. Frizzi, J. C. Dehaes, and A. Dubus, "Prompt gamma imaging with a slit camera for real-time range control in proton therapy," *Phys. Med. Biol.*, vol. 57, no. 11, p. 3371, 2012. [Online]. Available: <http://dx.doi.org/10.1088/0031-9155/57/11/3371>